JLAB-THY-11-1372
INT-PUB-11-020

The Role of the Roper in Chiral Perturbation Theory

Bingwei Long

Excited Baryon Analysis Center (EBAC),

Jefferson Laboratory, 12000 Jefferson Avenue,

Newport News, Virginia 23606, USA and

European Centre for Theoretical Studies in Nuclear Physics

and Related Areas (ECT), I-38123 Villazzano (TN), Italy*

U. van Kolck

Department of Physics, University of Arizona, Tucson, Arizona 85721, USA and

Instituto de Física Teórica, Universidade Estadual Paulista,

Rua Dr. Bento Teobaldo Ferraz, 271 - Bloco II, 01140-070, São Paulo, Brazil

(Dated: January 20, 2013)

arXiv:1105.2764v2 [nucl-th] 18 Oct 2011

Abstract

We include the Roper excitation of the nucleon in a version of heavy-baryon chiral perturbation theory recently developed for energies around the delta resonance. We find significant improvement in the P_{11} channel.

Chiral perturbation theory (ChPT) is the effective field theory (EFT) of QCD at momenta comparable to the pion mass, m_π. It includes the lightest hadron, the pion, but not mesons — such as the rho— with masses of the order of the typical QCD mass scale, $M_{\rm QCD} \sim 1$ GeV. The mesonic version of the theory [1] can be thought of as an expansion of amplitudes in $m_\pi/M_{\rm QCD}$ and $Q/M_{\rm QCD}$, where Q is a characteristic external momentum. This approach has been shown to be very successful [2] for a variety of processes at energies below a structure associated with the sigma meson at a position $m_\sigma - i\Gamma_\sigma/2 = (441 - 272i)$ MeV [3] in the complex energy plane, which suggests a radius of convergence $\Sigma \sim \sqrt{m_\sigma^2 + \Gamma_\sigma^2/4} \simeq 6f_\pi$, where $f_\pi \simeq 92$ MeV is the pion decay.

ChPT includes also the lightest baryon, the nucleon, because the relatively large nucleon mass, m_N, is inert in low-energy process [4]. However, contrary to the mesonic sector, the first baryon excitations appear at energies not much larger (relative to m_N) than m_π. The most important is the delta isobar at $m_\Delta - m_N - i\Gamma_\Delta/2 \simeq (270 - 50i)$ MeV [5]. If the delta is not included explicitly, the theory represents an expansion in $\sim (Q, m_\pi)/\delta$ with $\delta \equiv m_\Delta - m_N \simeq 3f_\pi$, which cannot be applied at energies much beyond the threshold region. The importance of the delta in ChPT has been recognized for a long time, and introducing a field to describe its long-distance effects rearranges ChPT contributions and improves its convergence pattern [6–8]. In order to calculate amplitudes in the vicinity of δ, a selective resummation is required [9, 10]. Generally this yields very good results [11, 12]. In the quintessential low-energy nucleon reaction, elastic πN scattering, the leading delta contribution is of $\mathcal{O}(M_{\rm QCD}^2/Q)$, in contrast with ChPT near threshold [2] where "leading order" is used to refer to $\mathcal{O}(Q)$. All channels except P_{11} are well described at $\mathcal{O}(Q)$ [10], which here means next-to-next-to-leading order.

Other nucleon excitations have received considerably less attention in ChPT. Among them, the Roper [13] is special, and here we argue that the Roper can be considered within the regime of ChPT, although of course in a marginal sense. First, the Roper pole appears at an energy not very far above the delta, $m_R - m_N - i\Gamma_R/2 \simeq (420 - 80i)$ MeV [5]. Without explicit Roper contributions, the theory is as an expansion in $\sim (Q, m_\pi)/\rho$, where Q now includes δ, and $\rho \equiv m_R - m_N \simeq 4.5f_\pi$. Other resonances lay at least Σ above threshold (for example, the next higher S_{11} resonance has a larger mass, $m_{S_{11}} - m_N \gtrsim 6f_\pi \simeq \Sigma$ [5]), and it is difficult to see how they could be incorporated in the EFT without the concomitant inclusion of meson resonances. Second, the Roper width is $\Gamma_R \sim \Gamma_\Delta \rho^3/2\delta^3$, as expected from ChPT widths that scale as $Q^3/M_{\rm QCD}^2$. The same is not true for higher resonances, which typically have smaller relative widths. Third, the delta and the Roper nearly saturate the Adler-Weisberger sum rule, a result which suggests that, together with the nucleon, these two resonances fall into a simple reducible representation of the chiral

$SU(2)_L \times SU(2)_R$ group [14, 15].

The Roper could thus be expected to play a role in low-energy observables. Take, for example, elastic πN scattering in the P_{11} channel. The phase shift [5] is repulsive near threshold but becomes attractive at a center-of-mass (CM) energy (with m_N subtracted out) $E \sim 3f_\pi$, right in the delta region. In ChPT, whether without [16–19] or with [10, 20–22] an explicit delta, the near-threshold behavior is reproduced in lowest orders with a monotonically decreasing phase shift. The turnaround can at best be achieved if a nominally higher-order effect provides an opposite contribution to the lower orders. This is not a problem when this region is considered beyond the range of EFT, but needs to be addressed as we extend this range, as done in Refs. [9–12]. The attraction in this channel has long been identified as due to the Roper, thanks to its relatively low position and large width.

In this article we incorporate the Roper in ChPT, leading to an expansion in $\sim (Q, m_\pi)/\Sigma$, where Q now includes ρ as well. We continue to refer to this EFT as ChPT because it still relies on expansions in the quark masses and in momenta. We illustrate its effect in elastic πN scattering. We consider $E \sim \delta$ and show that the Roper pole diagram is enhanced, significantly improving the description of the P_{11} channel at the first non-vanishing order, $\mathcal{O}(Q)$. We check explicitly that this description is preserved at next order, $\mathcal{O}(Q^2/M_{\rm QCD})$. We refrain in this first approach from pushing the theory to $E \sim \rho$. At such energies a resummation is necessary, just like that in the P_{33} channel at $E \sim \delta$. However, the proximity to the scale where other effects (σ, $N^\star(1520)$, $N^\star(1535)$) accumulate is likely to lead to slow convergence. Nevertheless, since the Roper lies not far from the delta and its width is large, its effects are felt long before $E \sim \rho$.

Aspects of Roper physics —the m_π dependence of its mass and width— have already been considered in ChPT [23] with an eye to lattice extrapolations. The role of the Roper and other resonances on the properties of the baryon decuplet has been discussed in $SU(3)$ ChPT [24]. An early study of the Roper in πN scattering appeared in Ref. [20], although no considerations of power counting guided the selection of contributions. Note that other approaches exist to incorporate the Roper (and other resonances) consistently with chiral symmetry and field-definition independence. They are reminiscent of the original approach [8, 25] to nuclear interactions using a chiral Lagrangian: a pion-nucleon "kernel" is first derived in ChPT to a certain order and then unitarized, for example using the N/D method [19, 26] or the Bethe-Salpeter equation [27]. (Similar approaches based on meson-exchange models include those in Ref. [28].) Power counting is not manifest at the amplitude level, but good results for pion-nucleon phase shifts are obtained into the Roper region. Needless to say, the Roper has long been been shown to be important in phenomenological hadronic models [29]. For a recent review of Roper properties, see Ref. [30].

The EFT contains all interactions allowed by the symmetries of QCD. The chiral Lagrangian with pion ($\boldsymbol{\pi}$), nucleon (N) and delta (Δ) fields that is required for πN scattering up to $\mathcal{O}(Q^2/M_{\mathrm{QCD}})$ in the channel of interest is given in Refs. [6–8, 10]. We adopt for definiteness the chiral Lagrangian in the form of Ref. [10], and enlarge it by introducing a heavy-Roper field (R) with the same quantum numbers as the nucleon. Since approximate $SU(2)_L \times SU(2)_R$ chiral symmetry can be accounted in EFT through a non-linear realization based on unbroken isospin, the technology to construct interactions involving this field is the same as for the nucleon. The Lagrangian terms can be organized according to the chiral index $\nu = d + m + n_\delta + n_\rho + f/2 - 2 \geqslant 0$ of an interaction, where d, m, n_δ, n_ρ and f count derivatives, powers of m_π, powers of δ, powers of ρ, and number of baryon fields, respectively. In the following we will need explicitly only the lowest-index Lagrangian,

$$\begin{aligned}\mathcal{L}^{(0)} = {} & 2f_\pi^2 \boldsymbol{D}^2 - \frac{m_\pi^2}{2}\frac{\boldsymbol{\pi}^2}{(1+\boldsymbol{\pi}^2/4f_\pi^2)} + N^\dagger i\mathscr{D}_0 N + g_A N^\dagger \boldsymbol{\tau}\vec{\sigma} N \boldsymbol{\cdot}\cdot \vec{\boldsymbol{D}} \\ & + \Delta^\dagger \left(i\mathscr{D}_0 - \delta\right)\Delta + h_A \left(N^\dagger \boldsymbol{T}\vec{S}\Delta + H.c.\right) \boldsymbol{\cdot}\cdot \vec{\boldsymbol{D}} \\ & + R^\dagger \left(i\mathscr{D}_0 - \rho\right) R + g_A' \left(N^\dagger \boldsymbol{\tau}\vec{\sigma} R + H.c.\right) \boldsymbol{\cdot}\cdot \vec{\boldsymbol{D}} + \cdots \ ,\end{aligned} \tag{1}$$

and its first correction

$$\begin{aligned}\mathcal{L}^{(1)} = {} & N^\dagger \left(\frac{\vec{\mathscr{D}}^2}{2m_N} + B_2 \vec{\boldsymbol{D}} \cdot \vec{\boldsymbol{D}} + B_3 \varepsilon_{abc}\varepsilon_{ijk} D_{ai} D_{bj} \tau_c \sigma_k\right) N + \frac{1}{2m_N}\Delta^\dagger \vec{\mathscr{D}}^2 \Delta + \frac{1}{2m_N} R^\dagger \vec{\mathscr{D}}^2 R \\ & - \frac{g_A}{2m_N}\left(iN^\dagger \boldsymbol{\tau}\vec{\sigma}\cdot\vec{\mathscr{D}} N + H.c.\right) \boldsymbol{\cdot} \boldsymbol{D}_0 - \frac{h_A}{m_N}\left(iN^\dagger \boldsymbol{T}\vec{S}\cdot\vec{\mathscr{D}}\Delta + H.c.\right) \boldsymbol{\cdot} \boldsymbol{D}_0 \\ & - \frac{g_A'}{m_N}\left(iN^\dagger \boldsymbol{\tau}\vec{\sigma}\cdot\vec{\mathscr{D}} R + H.c.\right) \boldsymbol{\cdot} \boldsymbol{D}_0 + \cdots \ .\end{aligned} \tag{2}$$

Here $\boldsymbol{D}_\mu = \partial_\mu \boldsymbol{\pi}/2f_\pi + \ldots$ and $\mathscr{D}_\mu = \partial_\mu + i\boldsymbol{t}^{(I)} \cdot (\boldsymbol{\pi} \times \boldsymbol{D}_\mu)/f_\pi$ are the pion and baryon chiral-covariant derivatives; $\boldsymbol{t}^{(I)}$ is the isospin generator in a representation of isospin I; $\vec{\sigma}$ and $\boldsymbol{\tau} = 2\boldsymbol{t}^{(1/2)}$ are the Pauli matrices in spin and isospin; $\vec{S}$ and $\boldsymbol{T}$ are 2×4 transition matrices in spin and isospin, normalized so that $S_i {S_j}^\dagger = \left(2\delta_{ij} - i\epsilon_{ijk}\sigma_k\right)/3$ and analogously for $\boldsymbol{T}$; g_A, h_A, and g_A' are the leading coupling constants of the pion with the nucleon, nucleon-delta, and nucleon-Roper, respectively; and $B_{2,3}$ are low-energy constants (LECs) of $\mathcal{O}(1/M_{\mathrm{QCD}})$. For simplicity we work here in the isospin-symmetric limit, although (generically small) isospin breaking can be introduced along the lines of Ref. [8].

Contributions to an arbitrary low-energy process can be ordered in powers of $Q/M_{hi} \sim M_{lo}/M_{hi}$, where $M_{lo} \sim m_\pi \sim \delta \sim \rho < M_{hi} \sim \Sigma \lesssim M_{\mathrm{QCD}}$. Throughout the low-energy region the standard ChPT power counting [1] applies. In the near-threshold region, the theory is purely perturbative in powers of Q/M_{hi}. In a region $|E-\delta| = \mathcal{O}(\delta^3/M_{hi}^2)$ around the delta pole, there is a "kinematic" fine-tuning: one-delta-reducible contributions are enhanced and the delta self-energy needs to be resummed [10] (and, for a slightly different, earlier version, [9]). At $\mathcal{O}(M_{hi}^2/Q)$ the πN amplitude is non-zero only in the P_{33} channel, where it has a standard Breit-Wigner form with a constant width. At $\mathcal{O}(Q)$, the width acquires an energy dependence, and an energy-dependent background appears in all S and P waves, stemming from standard tree diagrams without a delta pole. Using $m_\pi = 139$ MeV, $m_N = 939$ MeV, $f_\pi = 92.4$ MeV, and $g_A = 1.29$ as input, we find [10] a very good fit to P_{33} phase shifts [5] with $\delta = 305$ MeV and $h_A = 2.92$. Thus, h_A/g_A is not far from the large-N_c value $3/\sqrt{2}$ [31]. The resulting P_{13} and P_{31} phases are equal [10], in qualitative, and at low energies reasonably quantitative, agreement with the corresponding observed phase shifts [5]. Thus, ChPT can be successfully extended beyond $E \sim \delta$.

Now consider the effects of the Roper. The dominant Roper contributions will generically be the tree diagrams in FIG. 1. More complicated diagrams, involving more derivatives and/or loops, should be suppressed by powers of Q/M_{hi}, and, barring fine-tuning, be of higher orders. The dominant diagrams themselves, if the Roper is integrated out, would contribute to the "seagull" counterterms, $\pi\pi\bar{N}N$, in the sub-leading Lagrangians of the Roperless EFT. Their contributions would appear together with others of $\mathcal{O}(Q^2/M_{hi})$. The Roper crossed diagram is indeed of this order: it decreases with energy and is, at $E \sim \delta$,

$$\frac{Q^2}{E+\rho} \sim \frac{Q^2}{\delta+\rho} \sim \frac{Q^2}{M_{hi}} \; . \tag{3}$$

However, the Roper pole diagram increases in importance as the energy increases and at $E \sim \delta$ is

$$\frac{Q^2}{E-\rho} \sim \frac{Q^2}{\delta-\rho} \sim \frac{Q^2}{M_{lo}} \; . \tag{4}$$

Because the Roper and the delta are not widely separated, the first Roper contribution in the delta region is not suppressed by a large scale M_{hi}, but by the small scale M_{lo}. The size of this contribution is $\mathcal{O}(Q)$, not $\mathcal{O}(Q^2/M_{\mathrm{QCD}})$. It is comparable to the nucleon pole and crossed diagrams,

$$\frac{Q^2}{E} \sim \frac{Q^2}{\delta} \sim \frac{Q^2}{M_{lo}} \; , \tag{5}$$

and to the delta crossed diagram

$$\frac{Q^2}{E+\delta} \sim \frac{Q^2}{2\delta} \sim \frac{Q^2}{M_{lo}} \; . \tag{6}$$

Near threshold, $E \sim m_\pi$, this counting overestimates the Roper and delta effects due to the numerical difference between $\rho - m_\pi$ and $\delta + m_\pi$, on the one hand, and m_π on the other.

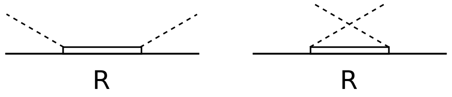

FIG. 1: Roper pole and crossed tree diagrams. A double solid line marked "R" represents a Roper, a single solid line a nucleon, and a dashed line a pion.

As E increases further and enters a window of size $|E-\rho| = \mathcal{O}(\rho^3/M_{hi}^2)$ around the Roper pole, the Roper-pole diagram becomes $\mathcal{O}(M_{hi}^2/Q)$ and the Roper self-energy is comparable to $|E-\rho|$. In this window one-Roper-irreducible diagrams require the same treatment as for the delta in Ref. [10]. At $\mathcal{O}(M_{hi}^2/Q)$, the Roper self-energy is made of one-loop diagrams that should be resummed. Already at $\mathcal{O}(Q)$, however, complicated two-loop diagrams appear which account for the Roper decay into two pions. Although this decay mode is significant, it is still less important than decay into a single pion [32]. This suggests that the EFT expansion could work even in this region, but we defer a detailed study of πN scattering at the less favorable energy $E \sim \rho$ to a later publication.

Outside this window, the Roper pole diagram should capture the dominant part of the rise of the resonance, and is the only Roper effect that needs to be considered to $\mathcal{O}(Q)$, or N^{2}LO. In πN scattering, it contributes only to the P_{11} channel. The inclusion of an explicit Roper does not modify the amplitudes in the other P-wave channels, and therefore does not spoil the good description found in Ref. [10]. This special treatment of the Roper is different from the way the delta is dealt with in Ref. [10]. It enables us to improve the description of P_{11} over Ref. [10] with minimal complication, provided that one stays below the Roper, $E \sim \delta < \rho$. In this region an extension to higher orders poses no significant problems, although at some order of course two-loop diagrams also appear. Whether the relatively slow convergence of the width will translate into a slow convergence of the full loop expansion at low energies remains to be seen.

To see the dominant Roper effects, we work with πN scattering in the CM frame, and denote by k the magnitude of the pion momentum, by $\omega = \sqrt{k^2 + m_\pi^2}$ its energy, and by $W_{\mathrm{CM}} \equiv m_N + E$ the total CM energy. For $E \sim \delta$, the first non-vanishing contributions in the P_{11} channel are given by the nucleon pole and crossed diagrams, the delta crossed diagram, and the Roper pole diagram (see FIG. 2), all constructed entirely from $\mathcal{L}^{(0)}$, Eq. (1). We find for the first non-vanishing contributions to the T matrix in the P_{11} channel

$$T_{P_{11}}^{\mathrm{N^2LO}} = -\frac{g_A^2}{3\pi f_\pi^2} k^3 \mathcal{N}(k) \left[\frac{1}{E} - \left(\frac{\sqrt{2} h_A}{3 g_A} \right)^2 \frac{1}{E+\delta} + \frac{9}{8} \left(\frac{g_A'}{g_A} \right)^2 \frac{1}{E-\rho} \right] , \tag{7}$$

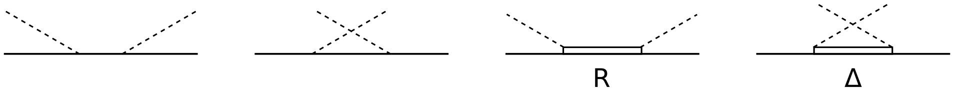

FIG. 2: N^{2}LO diagrams. Vertices have $\nu = 0$. A double solid line marked "Δ" represents a delta isobar; other notation as in FIG. 1.

where

$$\mathcal{N}(k) \equiv \frac{1 + (E - \omega)/m_N}{1 + E/m_N} \tag{8}$$

is a kinematic coefficient. Here the nucleon and delta terms are the same as in Ref. [10]. Since the relative coefficient of the delta contribution is $\simeq 1$, the nucleon contribution is numerically larger and leads (in the absence of the Roper term) to repulsive phase shifts throughout the low-energy region. As long as $(g'_A/g_A)^2$ is not too large, this situation survives near threshold. As E increases, however, while (apart from the overall k^3) the nucleon and delta contributions decrease in magnitude, the Roper contribution increases. Since it has sign opposite to the nucleon term as long as $E < \rho$, it will eventually overcome the others. As long as $(g'_A/g_A)^2$ is not too small, this happens at energies $E \sim M_{lo}$.

In next order, $\mathcal{O}(Q^2/M_{hi})$ or N^{3}LO, there are more tree-level contributions, see FIG. 3. In addition to the Roper crossed diagram (a), these contributions stem from one insertion of terms in $\mathcal{L}^{(1)}$, Eq. (2): nucleon recoil (b, c) and the Galilean pion-nucleon vertex correction (d, e) in nucleon pole and crossed diagrams; delta recoil (f) and the Galilean pion-nucleon-delta vertex correction (g) in delta crossed diagrams; Roper recoil (h) and the Galilean pion-nucleon-Roper vertex correction (i) in Roper pole diagrams; and pion-nucleon seagulls (j). Of these diagrams, (b), (h) and (i) vanish in the CM frame, and (c) and (f) do not contribute to the P_{11} partial wave. We find

$$T^{\mathrm{N^3LO}}_{P_{11}} = -\frac{g_A^2}{3\pi f_\pi^2} k^3 \mathcal{N}(k) \left[\frac{\omega}{E\, m_N} - \left(\frac{\sqrt{2} h_A}{3 g_A}\right)^2 \frac{2\omega}{(E+\delta) m_N} - \frac{1}{8}\left(\frac{g'_A}{g_A}\right)^2 \frac{1}{E+\rho} + \frac{B}{g_A^2} \right] , \tag{9}$$

where

$$B = B_3 - \frac{B_2}{4} - \frac{1}{4 m_N} \tag{10}$$

in terms of the LECs $B_{2,3}$. The nucleon contributions in Eqs. (7) and (9) are in agreement with Ref. [17]. While Eq. (7) agrees with the $\mathcal{O}(Q)$ delta contributions in Ref. [22], a comparison at $\mathcal{O}(Q^2)$ is obscured by the employment in Ref. [22] of off-shell parameters and a $\nu = 1$ $\pi N \Delta$ coupling, $b_3 + b_8$, which is removed in our calculation using integration by parts and baryonic equations of motion [33]. To this order, our EFT resembles an isobar model such as that in Ref. [29], the main

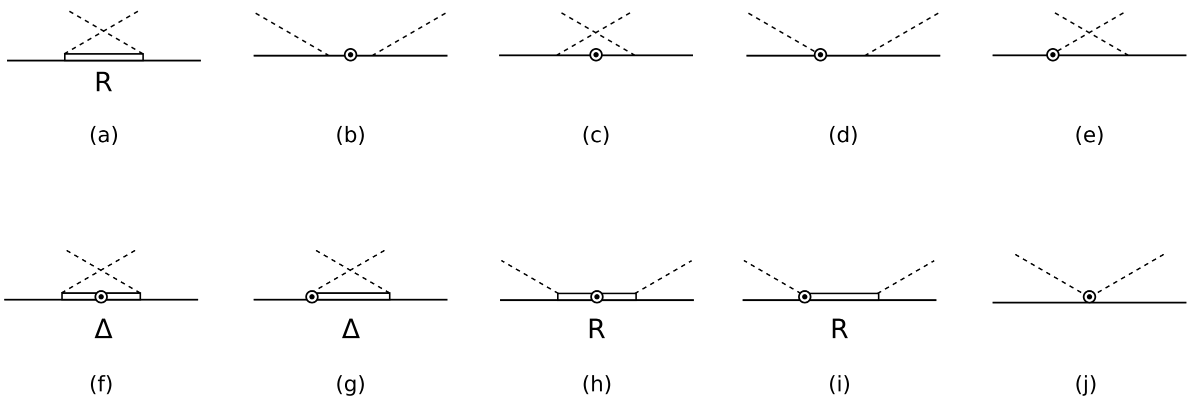

FIG. 3: $\mathrm{N^3LO}$ diagrams. Once-circled vertices have $\nu = 1$; other notation as in FIG. 1 and FIG. 2. Diagrams with the same topology but different permutation of vertices are drawn only once.

difference lying on the B term. Such term accounts for the short-range physics not considered explicitly in ChPT. Although unknown, it is not completely free: for the EFT expansion to be sensible, B is expected to be naturally sized, $B \sim 1/M_{hi}$. Pion loops and further LECs appear in sub-leading orders.

Expanding also the phase shifts in powers of Q/M_{hi}, they can be extracted from Eqs. (7) and (9) in such a way that unitarity is preserved perturbatively: $\theta_{P_{11}}^{\mathrm{N^2LO}} = T_{P_{11}}^{\mathrm{N^2LO}}/2$ and $\theta_{P_{11}}^{\mathrm{N^3LO}} = T_{P_{11}}^{\mathrm{N^3LO}}/2$. If we use the same nucleon and delta parameters determined at $\mathrm{N^2LO}$ in Ref. [10], we have just two undetermined parameters at $\mathrm{N^2LO}$, ρ and g_A', and one more at $\mathrm{N^3LO}$, B. We fit our results to the P_{11} phases from the energy-dependent solution of the phase-shift analysis (PSA) by the George Washington (GW) group [5].

The P_{11} phase shifts have an interesting feature: they almost vanish until reaching the sign-flip point, $E \sim \delta$, beyond which they become attractive. The phase is only about -1° at the lowest point of the "dip". This suggests that, for a wide kinematic window, the repulsion contributed by the nucleon nearly cancels the attraction by the delta and Roper. This sort of cancellation stands out among the low-energy S and P partial waves. While the sign-flip point constrains ρ and g_A' at $\mathrm{N^2LO}$ (Eq. (7)), the near cancellation for a wide window implies that the constraint is not restrictive at all, within an error of 1°. Thus, we expect a significant uncertainty in determining ρ or g_A'. We reduce this uncertainty by fitting points on the right side of the sign-flip point, from $W_{\mathrm{CM}} = 1250$ MeV to 1300 MeV, where the phase shifts become appreciable. Since the energy-dependent solution of the GW PSA does not have error bars, each input PSA point is fitted with the same weight, and only the central values of the LECs are shown below.

The results for the P_{11} phase shifts are shown in the left plot of FIG. 4. For most of the plot,

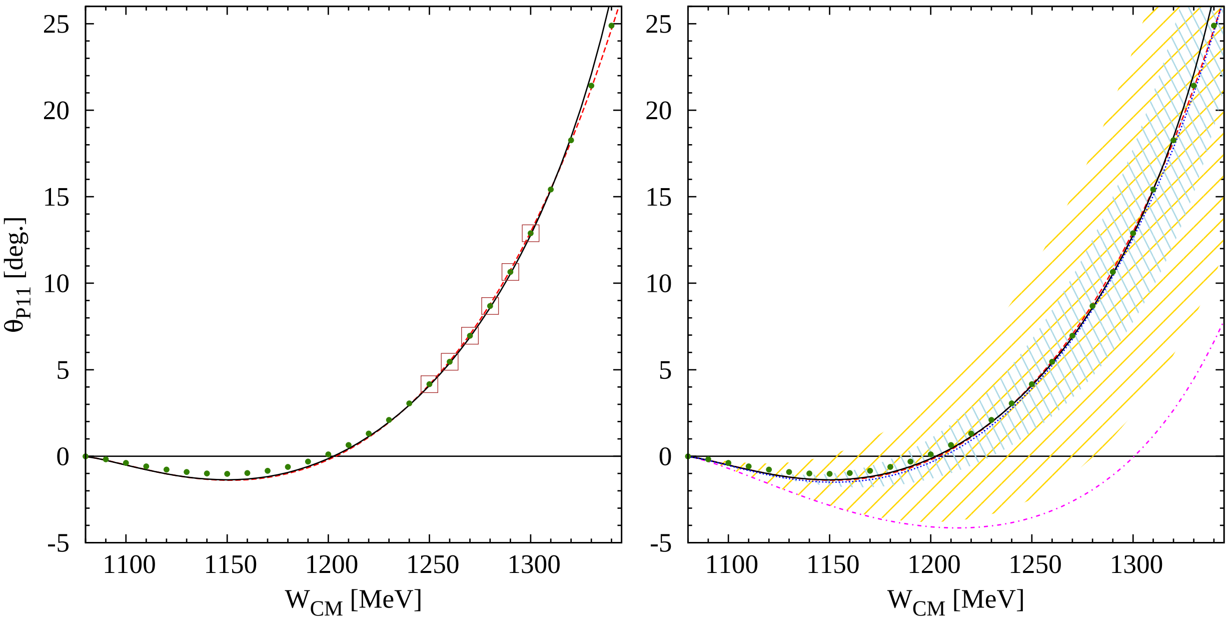

FIG. 4: The P_{11} phase shift $\theta_{P_{11}}$ as a function of $W_{\rm CM}$, the CM energy including the nucleon mass. LO and NLO vanish in this channel; the $\rm N^2LO$ EFT fit is given by the (red) dashed line and the $\rm N^3LO$, by the (black) solid line. The green dots are the results of the GW phase-shift analysis [5]. On the left plot, the PSA points used as input in the EFT fit are marked by square boxes. On the right plot, the theoretical error band at $\rm N^2LO$ is indicated by a (gold) forward hatched area, and at $\rm N^3LO$ by a (light blue) backward hatched area. We also show as, respectively, (magenta) dot-dashed and (blue) dotted curves the $\rm N^2LO$ and $\rm N^3LO$ results using as input the Breit-Wigner mass and width from the GW analysis [5].

the $\rm N^3LO$ curve coincides with the $\rm N^2LO$ curve. It fits slightly worse on the uphill to the Roper resonance, but does slightly better in the region we take the PSA inputs. The two curves agree with each other and data much more than one would expect. The theoretical error of the EFT amplitudes can be estimated as follows: (*i*) at $\rm N^2LO$,

$$\Delta T^{\rm N^2LO}_{P_{11}} = \pm \frac{k^2 \mathcal{N}(k)}{3\pi f_\pi^2}\frac{k}{M_{hi}}\,, \tag{11}$$

which can be interpreted as the πN seagull terms with a "natural" size; (*ii*) at $\rm N^3LO$,

$$\Delta T^{\rm N^3LO}_{P_{11}} = \pm \frac{k^2 \mathcal{N}(k)}{3\pi f_\pi^2}\frac{k^2}{M_{hi}^2}\,. \tag{12}$$

The theoretical errors, with $M_{hi} = 600$ MeV, are indicated by shaded areas in the right plot of FIG. 4.

From the fit we extract values for ρ, g'_A, and B. These are given in the first two rows of TABLE I, together with values for δ and h_A found in Ref. [10], and the value of g_A used as input. These are the values that give the curves in the left panel of FIG. 4. In order to have an estimate of the

TABLE I: Low-energy constants appearing in the P_{11} channel up to N^{3}LO encoding nucleon (g_A), delta (h_A and δ, in MeV), Roper (g'_A and ρ, in MeV), and higher-energy (B, in GeV^{-1}) properties. The values for g'_A, ρ and B extracted from the EFT fits at N^{2}LO and N^{3}LO (where g_A, h_A, and δ were used as input) are labeled "EFT". In the rows labeled "GW", ρ and g'_A are extracted from the Breit-Wigner parameters for the Roper [5]. The values when the nucleon, delta and Roper form a reducible representation of chiral symmetry with maximal mixing [15] are labeled "Chiral rep".

	g_A	h_A	δ (MeV)	g'_A	ρ (MeV)	B (GeV^{-1})
N^{2}LO EFT	1.29	2.92	305	1.06	690	—
N^{3}LO EFT	1.29	2.92	305	0.32	470	−2.3
N^{2}LO GW	1.29	2.92	305	0.54	550	—
N^{3}LO GW	1.29	2.92	305	0.54	550	−1.6
Chiral rep	1.33	2.82	292	0.33	527	—

uncertainty in a LEC, we consider its variation so that the EFT curves roughly stay, up to 1300 MeV, within the theoretical error band in the right panel of FIG. 4, while other LECs are fixed at central values. At N^{3}LO, we find $g'_A = 0.32^{+0.14}_{-0.18}$, $\rho = 470^{+250}_{-40}$ MeV, and $B = -2.3^{+0.7}_{-0.7}$ GeV^{-1}. Of course, the errors in the parameters are correlated and these variations are just an illustration of the uncertainty in the parameter-space region that generates the extreme curves. These results are compared to values, in the last row, from the assumption that the nucleon, delta, and Roper form a reducible representation of chiral symmetry with maximal mixing [15]. At N^{3}LO there is agreement better than 15% for central values, well within the errors of the N^{3}LO extraction. (Note that the signs of h_A and g'_A cannot be extracted from our analysis, and were simply chosen to be the same as in Ref. [15].)

Although the two fitted phase-shift curves almost coincide, we should not conclude that the EFT expansion in P_{11} converges very rapidly. The relatively large variation of ρ and g'_A from N^{2}LO to N^{3}LO shows the significant impact of the N^{3}LO correction. Because B is still naturally sized, $\mathcal{O}(1/M_{\mathrm{QCD}})$, the N^{3}LO amplitude (Eq. (9)) is one order of magnitude smaller than the magnitude of either the repulsive or the attractive term at N^{2}LO (Eq. (7)). But, in order for the sum of two orders to nearly vanish below $E \simeq \delta$, the N^{2}LO and its subleading corrections need to be numerically comparable, which indicates slow convergence of the EFT expansion in this channel. However, the overall convergence is reasonable in the sense that the N^{3}LO P_{11} is still one order smaller than, e.g., the P_{33} N^{2}LO amplitude [10].

The large change in Roper parameters from one order to the next is consequence of fitting them away from the Roper resonance region, which is most sensitive to them. In order to have another estimate of uncertainties and convergence, we consider an alternative way to determine the Roper parameters. The leading πN partial width of the Roper is

$$\Gamma^{(0)}_{\pi N}(E) = \frac{3}{8\pi}\left(\frac{g'_A}{f_\pi}\right)^2 \mathcal{N}(k_\rho) k_\rho^3\,, \tag{13}$$

where k_ρ is the CM momentum when the Roper is on-shell. When we fit ρ and g'_A to the Breit-Wigner mass and width from GW PSA [5], and at N^{3}LO B from the same phases as before, we obtain two extra curves shown in the right panel of FIG. 4. The parameters obtained this way are shown in the rows of TABLE I labeled "GW". Although the values of ρ and g'_A extracted from the Breit-Wigner resonance parameters appear quite different from those fitted at N^{2}LO, the phenomenological curve is in the vicinity of the N^{2}LO error band, which confirms the difficulty in extracting ρ and g'_A from the EFT amplitude at N^{2}LO. The smaller error band at N^{3}LO suggests a more reliable extraction of LECs: ρ indeed has come closer to the Breit-Wigner mass or the real part of the Roper pole position. The large variation in the "GW" curves from N^{2}LO to N^{3}LO is a reflection of the importance of the background (here represented by the LEC B), which in turn is another consequence of slow convergence. Note that we use this procedure based on Breit-Wigner parameters only as an illustration that our Roper N^{3}LO values might survive an extension of the theory to the Roper region; we cannot, and do not, make claims about the success of an eventual fit in this region.

Although we do not aim at a precise description of the threshold region, we extract for completeness the corresponding scattering volume at N^{3}LO:

$$\begin{aligned} a_{P_{11}} = -\frac{g_A^2}{6\pi f_\pi^2 m_\pi}\Bigg\{ 1 - \left(\frac{\sqrt{2}h_A}{3g_A}\right)^2 \frac{m_\pi/\delta}{1+m_\pi/\delta}\,\frac{1+2m_\pi/m_N}{1+m_\pi/m_N} \\ - \left[\frac{5}{4}\left(\frac{g'_A}{g_A}\right)^2 \frac{m_\pi}{\rho}\,\frac{1+4m_\pi/5\rho}{1-m_\pi^2/\rho^2} - \frac{m_\pi B}{g_A^2}\right]\left(1+\frac{m_\pi}{m_N}\right)^{-1}\Bigg\}\,. \end{aligned} \tag{14}$$

The delta and Roper contributions are suppressed by factors of m_π/δ and m_π/ρ, respectively. With the N^{3}LO EFT values of ρ and g'_A in TABLE I, the delta, Roper and seagull counterterm contributions are, respectively, -40%, -2.7% and -17% of the nucleon's, and $a_{P_{11}} = -0.081\, m_\pi^{-3}$, in a good agreement with $a_{P_{11}} = -(0.0799 \pm 0.0016) m_\pi^{-3}$ found in a PSA based on low-energy data [34]. Of course, the successful description near threshold owes more to the seagull than to the Roper. The scattering length can be fitted in Roperless, deltaless ChPT with an effective B_{eff} that accounts for the delta, Roper, and higher-energy contributions. It is reassuring that parameters fitted at $E \sim \delta$ produce nearly the same value for B_{eff}, the expression of which to N^{3}LO in our EFT can be directly read off Eq. (14).

In summary, we have argued that the Roper can profitably be included in ChPT. As a first study, we focused on πN scattering below the Roper resonance, in the region around the delta. We proposed the promotion of the Roper pole diagram over its crossed counterpart. Using this counting scheme, we found a good description of the P_{11} phase shifts throughout the low-energy region already at lowest non-vanishing order. The smallness of the P_{11} phase shifts at low energies makes difficult a reliable extraction of LECs from the EFT amplitude at this order, but at next order the best fit gives LECs close to those predicted by a reducible chiral representation with maximal mixing. The cancellations necessary for small P_{11} phase shifts suggest a slow convergence at low orders in the P_{11} channel, but it does not spoil overall convergence, when all partial waves, including those of more natural size, are taken into account.

Acknowledgments

We thank Silas Beane for useful comments. We are grateful to the following institutions for hospitality while this work was being carried out: the Kernfysisch Versneller Instituut at Rijksuniversiteit Groningen (UvK), the National Institute for Nuclear Theory at the University of Washington (BwL, UvK), and the University of Arizona (BwL). This work was supported by the US DOE under contracts DE-AC05-06OR23177 (BwL) and DE-FG02-04ER41338 (UvK). This work is coauthored by Jefferson Science Associates, LLC under US DOE Contract No. DE-AC05-06OR23177.

---

[1] S. Weinberg, *Physica* **96A** (1979) 327; J. Gasser and H. Leutwyler, *Ann. Phys.* **158** (1984) 142; *Nucl. Phys.* **B250** (1985) 465.

[2] V. Bernard, N. Kaiser, and U.-G. Meißner, *Int. J. Mod. Phys.* **E4** (1995) 193; V. Bernard, *Prog. Part. Nucl. Phys.* **60** (2008) 82.

[3] I. Caprini, G. Colangelo, and H. Leutwyler, *Phys. Rev. Lett.* **96** (2006) 132001.

[4] J. Gasser, M.E. Sainio, and A. Švarc, *Nucl. Phys.* **B307** (1989) 779; E. Jenkins and A.V. Manohar, *Phys. Lett.* **B255** (1991) 558.

[5] R.A. Arndt, W.J. Briscoe, I.I. Strakovsky, and R.L. Workman, *Phys. Rev.* **C74** (2006) 045205; R.A. Arndt *et al.*, The SAID program, `http://gwdac.phys.gwu.edu/`.

[6] E. Jenkins and A.V. Manohar, *Phys. Lett.* **B259** (1991) 353; in *Effective Field Theories of the Standard Model*, U.-G. Meißner (editor), World Scientific, Singapore (1992); E. Jenkins, *Nucl. Phys.* **B375** (1992) 561.

[7] T.R. Hemmert, B.R. Holstein, and J. Kambor, *Phys. Lett.* **B395** (1997) 89; *J. Phys.* **G24** (1998) 1831.

[8] U. van Kolck, Ph.D dissertation, U. of Texas (1993); C. Ordóñez, L. Ray, and U. van Kolck, *Phys. Rev. Lett.* **72** (1994) 1982; *Phys. Rev.* **C53** (1996) 2086; U. van Kolck, *Phys. Rev.* **C49** (1994) 2932; T.D. Cohen, J.L. Friar, G.A. Miller, and U. van Kolck, *Phys. Rev.* **C53** (1996) 2661.

[9] V. Pascalutsa and D.R. Phillips, *Phys. Rev.* **C67** (2003) 055202; V. Pascalutsa, *Prog. Part. Nucl. Phys.* **61** (2008) 27.

[10] Bingwei Long and U. van Kolck, *Nucl. Phys.* **A840** (2010) 39.

[11] V. Pascalutsa and M. Vanderhaeghen, *Phys. Rev. Lett.* **94** (2005) 102003; *Phys. Rev. Lett.* **95** (2005) 232001; *Phys. Rev.* **D73** (2006) 034003; *Phys. Rev.* **D77** (2008) 014027.

[12] V. Pascalutsa, M. Vanderhaeghen, and S.N. Yang, *Phys. Rept.* **437** (2007) 125.

[13] L.D. Roper, *Phys. Rev. Lett.* **12** (1964) 340.

[14] S. Weinberg, *Phys. Rev.* **177** (1969) 2604.

[15] S.R. Beane and U. van Kolck, *J. Phys.* **G31** (2005) 921.

[16] M. Mojžiš, *Eur. Phys. J.* **C2** (1998) 181.

[17] N. Fettes, U.-G. Meißner, and S. Steininger, *Nucl. Phys.* **A640** (1998) 199; N. Fettes and U.-G. Meißner, *Nucl. Phys.* **A676** (2000) 311; *Nucl. Phys.* **A693** (2001) 693.

[18] T. Becher and H. Leutwyler, *JHEP* **0106** (2001) 017.

[19] J.M. Alarcón, J. Martín Camalich, J.A. Oller, and L. Alvarez-Ruso, `arXiv:1102.1537`.

[20] A. Datta and S. Pakvasa, *Phys. Rev.* **D56** (1997) 4322.

[21] P.J. Ellis and H.-B. Tang, *Phys. Rev.* **C57** (1998) 3356; K. Torikoshi and P.J. Ellis, *Phys. Rev.* **C67** (2003) 015208.

[22] N. Fettes and U.-G. Meißner, *Nucl. Phys.* **A679** (2001) 629.

[23] B. Borasoy, P.C. Bruns, U.-G. Meißner, and R. Lewis, *Phys. Lett.* **B641** (2006) 294; D. Djukanovic, J. Gegelia, and S. Scherer, *Phys. Lett.* **B690** (2010) 123.

[24] M.K. Banerjee and J. Milana, *Phys. Rev.* **D54** (1996) 5804.

[25] S. Weinberg, *Phys. Lett.* **B251** (1990) 288; *Nucl. Phys.* **B363** (1991) 3.

[26] U.-G. Meißner and J.A. Oller, *Nucl. Phys.* **A673** (2000) 311.

[27] M.F.M. Lutz and E.E. Kolomeitsev, *Nucl. Phys.* **A700** (2002) 193.

[28] M. Döring, C. Hanhart, F. Huang, S. Krewald, and U.-G. Meißner, *Nucl. Phys.* **A829** (2009) 170; H. Kamano, S.X. Nakamura, T.-S.H. Lee, and T. Sato, *Phys. Rev.* **C81** (2010) 065207.

[29] E. Oset, H. Toki, and W. Weise, *Phys. Rept.* **83** (1982) 282; T. Ericson and W. Weise, *Pions and Nuclei*, Clarendon Press, Oxford, (1988).

[30] L. Alvarez-Ruso, arXiv:1011.0609 [nucl-th].

[31] A. Manohar, hep-ph/9802419.

[32] K. Nakamura [Particle Data Group], *J. Phys.* **G37** (2010) 075021.

[33] Bingwei Long and V. Lensky, *Phys. Rev.* **C83** (2011) 045206.

[34] E. Matsinos, W.S. Woolcock, G.C. Oades, G. Rasche, and A. Gashi, *Nucl. Phys.* **A778** (2006) 95.